CHEMISTRY
A EUROPEAN JOURNAL

DOI: 10.1002/chem.200800417

Tetraalkylammonium Salts of Weakly Coordinating Aluminates: Ionic Liquids, Materials for Electrochemical Applications and Useful Compounds for Anion Investigation

Ines Raabe,[b] Katrin Wagner,[a] Kristin Guttsche,[a] Mingkui Wang,[b] Michael Grätzel,[b] Gustavo Santiso-Quiñones,[a] and Ingo Krossing*[a]

Abstract: In this study, we investigated the tetraalkylammonium salts of the weakly coordinating fluorinated alkoxyaluminates [pftb]$^-$ ([Al(O(C-$(CF_3)_3)_4]^-$), [hfip]$^-$ ([Al(OC(H)-$(CF_3)_2)_4]^-$) and [hftb]$^-$ ([Al(OC(CH_3)-$(CF_3)_2)_4]^-$) in order to obtain information on their undisturbed spectral and structural properties, as well as to study their electrochemical behavior (i.e., conductivities in non-polar solvents and electrochemical windows). Several of the compounds qualify as ionic liquids with melting points as low as 42 °C for $[NBu_4]^+[hfip]^-$. Simple and almost quantitative metathesis reactions yielding these materials in high purity were developed. These $[NR_4]^+$ salts serve as model compounds for undisturbed anions and their vibrational spectra—together with simulated spectra based on quantum chemical DFT calculations—were used for the clear assignment of the anion bands. Besides, the ion volumes of the anions (V_{ion}-([pftb]$^-$)$=0.736$ nm^3, V_{ion}([hftb]$^-$)$=0.658$ nm^3, V_{ion}([hfip]$^-$)$=0.577$ nm^3) and their decomposition pathways in the mass spectrometric measurements have been established. The salts are highly soluble in non-polar solvents (up to 1.09 mol L^{-1} are possible for $[NBu_4]^+[hftb]^-$ in CH_2Cl_2 and 0.41 mol L^{-1} for $[NBu_4]^+[hfip]^-$ in $CHCl_3$) and show higher molar conductivities if compared to $[NBu_4]^+[PF_6]^-$. The electrochemical windows of CH_2Cl_2, CH_3CN and 1,2-$F_2C_6H_4$ using the $[NBu_4]^+$ aluminate electrolytes are up to $+0.5$ V/-0.7 V larger than those using the standard $[NBu_4]^+[PF_6]^-$.

Keywords: density functional calculations · electrochemistry · ionic liquids · tetraalkylammonium cations · weakly coordinating anions (WCAs)

Introduction

Tetraalkylammonium salts of complex anions play an important role especially in electrochemistry, where they are widely used as supporting electrolytes for applications like cyclic voltammetry in non-aqueous media.[1–6] However, the generated oxidized species often react with the anions and therefore, new salts with a large "electrochemical window" are required, that is, salts which are stable against oxidation and reduction under the experimental conditions, especially in low polarity solvents like CH_2Cl_2, $CHCl_3$ or toluene. Both requirements are fulfilled by quarterny ammonium salts of robust weakly coordinating anions (WCAs).[7] $[NBu_4]^+[B-(C_6F_5)_4]^-$ and $[NBu_4]^+[B(C_6H_3(CF_3)_2)_4]^-$ have been reported both to be very stable and to effectively solubilize the positively charged species formed in anodic processes.[8–12] However, electrochemical investigations in very non polar solvents like toluene or benzene are limited to only very few anions, for example, $[CB_{11}Me_{12}]^-$.[13,14] Unfortunately the synthesis of this anion is very complicated, which makes it impossible to be widely used as a WCA for electrochemical applications.

Quantum chemical calculations[15] as well as electrochemical measurements[16–20] of the lithium salts show the fluoroalkoxyaluminates [pftb]$^-$ ([Al(OC$(CF_3)_3)_4]^-$), [hftb]$^-$ ([Al(OC-$(CH_3)(CF_3)_2)_4]^-$) and [hfip]$^-$ ([Al(OC(H)$(CF_3)_2)_4]^-$) to be

[a] K. Wagner, K. Guttsche, Dr. G. Santiso-Quiñones, Prof. Dr. I. Krossing
Albert-Ludwigs-Universität Freiburg
Institut für Anorganische und Analytische Chemie
Albertstr. 21, 79104 Freiburg i. Br. (Germany)
Fax: (+49) 761 203 6001
E-mail: krossing@uni-freiburg.de

[b] Dr. I. Raabe, Dr. M. Wang, Prof. Dr. M. Grätzel
Ecole Polytechnique Fédérale de Lausanne
Institut des Sciences et Ingénierie Chimiques
EPFL-SB-ISIC-LPI, Station 6, 1015 Lausanne (Switzerland)

Supporting information for this article is available on the WWW under http://dx.doi.org/10.1002/chem.200800417: packing diagrams, crystal structures, solid state contacts, cyclovoltammograms, details on electrochemistry and crystallography.

very redox stable[1];[7,15,17] their salts are usually soluble in media with low dielectric constants (stability vs Li/Li^+ in DME: >5.0 V for $[hfip]^-$ and 5.5 V for $[pftb]^-$).

Moreover we have shown that even very reactive cations like simple carbenium ions (CI_3^+)[21,22] or reactive cations like PX_4^+,[23,24] $AsBr_4^+$,[25] $P_2X_5^+$,[23] $P_5X_2^+$,[23,26] $P_5S_2X_2^+$,[27] or $P_7S_6I_2^+$[28] (X = halogen) are compatible (i.e., could be stabilized) as salts of these aluminates. Especially the P–X cations are incompatible with all other anion types. This also holds for a series of silver and copper(I) complexes with very weakly basic ligands, for example, P_4,[29,30] P_4S_3,[31,32] S_8,[33] $P_3N_3Cl_6$,[34] or C_2H_4.[35,36] Since the starting materials to prepare compounds of the fluorinated aluminates are commercially available (best at P&M Invest Russia; http://www.fluorine.ru) and the synthesis of the lithium aluminate salts[37–39] is a simple high yield procedure that we have performed in scales up to 250 g per batch,[40] it only appeared logical to extend the available substance classes to $[NR_4]^+$ salts. During the preparation of this manuscript, an independent communication of the electrochemical windows of related compounds appeared.[41a,b]

Moreover, the $[NR_4]^+$ salts were used for the assignment of the ion volumes[42–44] and of the vibrational bands of the anions, as these compounds serve as model compounds for an undisturbed anion environment with all cation bands well known. The anion bands were assigned to the different vibrations by comparison to quantum chemical DFT calculations of the vibrational modes. The tetraalkylammonium salts were also chosen to investigate the anion decomposition pathways in the mass spectrometer by ESI techniques.

Results and Discussion

Syntheses: Two different strategies were used to prepare the tetraalkylammonium salts of the fluoroalkoxyaluminates: The $[NR_4]^+[pftb]^-$ salts (R = Bu **1**, Et **2**, Me **3**) were obtained by the reaction of $[NR_4]Br$ with Li[pftb] in a water/acetone mixture (85 vol %:15 vol %) according to the following Equation (1):

$$[NR_4]Br + Li[pftb] \xrightarrow{H_2O/acetone} [NR_4]^+[pftb]^- + LiBr \quad (1)$$

The $[NR_4]^+[pftb]^-$ formed is insoluble in pure water and crystallizes upon evaporation of the co-solvent acetone over night in quantitative yield. After several washings with water and testing for bromide with Ag^+, the compound is analytically pure (spectra, elemental analyses). Nevertheless, this method is only possible for the $[pftb]^-$ anion, as the other anions $[hftb]^-$ and $[hfip]^-$ are slightly sensitive towards moisture. Therefore, all of the other tetraalkylammonium compounds were synthesized in Et_2O/CH_2Cl_2 using the appropriate lithium salts [Eq. (2)].

$$[NR_4]Br + Li[A] \xrightarrow[2)\ CH_2Cl_2]{1)\ Et_2O} [NR_4][A] + LiBr \quad (2)$$
$$[A] = [hftb], [hfip]$$

The metathesis is performed in diethyl ether; however, to get rid of traces of dissolved $LiBr{\cdot}Et_2O$ complexes, the ether solvent is removed in vacuo and replaced by CH_2Cl_2, in which all the NR_4^+ aluminates are easily soluble. After filtration the pure compounds (spectra, elemental analyses) crystallize upon cooling the CH_2Cl_2 filtrate to 2 °C.

As seen from DSC measurements, the melting points of all $[hfip]^-$ and $[hftb]^-$ salts are rather low (between 42 and 110 °C, see Table 1), which qualifies most of them as ionic liquids (ILs), however, decomposition may start already below 200 °C, for example, $[NBu_4]^+[hfip]^-$ **4** decomposes at about 190 °C. By contrast, the salts of the $[pftb]^-$ anion are all thermally more stable but they also have much higher melting and decomposition points (for **2** and **3** > 400 °C).

Table 1. Melting points (T_m) and decomposition temperatures (T_d) of the NR_4^+ salts investigated in this study. Average values of two independently prepared batches (max. deviation: ±4 °C).

	T_m [°C]	T_d [°C]
$[NBu_4]^+[pftb]^-$ (**1**)	199	>250
$[NEt_4]^+[pftb]^-$ (**2**)	308	>400
$[NMe_4]^+[pftb]^-$ (**3**)	320	>400
$[NBu_4]^+[hfip]^-$ (**4**)	42	190
$[NEt_4]^+[hfip]^-$ (**5**)	56	>130
$[NMe_4]^+[hfip]^-$ (**6**)	61	147
$[NBu_4]^+[hftb]^-$ (**7**)	108	>150
$[NEt_4]^+[hftb]^-$ (**8**)	111	>230
$[NMe_4]^+[hftb]^-$ (**9**)	96	>150

Solid-state structures: For some of the $[NR_4]^+$ salts (**2**, **5**, **6**, **7**, and **9**), crystals suitable for X-ray diffraction could be obtained. The diffraction measurements were carried out at low temperatures (between 100 and 150 K) in order to minimize rotation of the CF_3 groups. In all of the solid-state structures, isolated cations and anions with only weak H···F contacts are found (see Supporting Information, where the cation–anion interactions are depicted). The crystal structure of $[NEt_4]^+[pftb]^-$ **2** shows no special or unexpected parameters and, therefore, will not be discussed here. A figure of **2** is deposited with the Supporting Information. For the $[hfip]^-$ and the $[hftp]^-$ anions, the tetraalkylammonium salts are the second examples of really ionic solid-state structures with isolated anions and cations,[41] while all the other species containing these anions, contain molecular structures with coordinated anions, for example, $[(P_4S_3)AgA]$,[31,32] $[(P_4)AgA]$,[45] $[(L)_2AgA]$,[35,46] or $[(L)AgA]$[35,46] ([A] = [hfip], [hftb], L = C_2H_2, C_2H_4). Therefore, the tetraalkylammonium salts of these anions serve as model compounds for undisturbed anions. Sections of the solid-state structures of one $[hfip]^-$ and one $[hftb]^-$ salt are shown in Figures 1 and 2, the other structures are deposited in the Supporting Information.

The most characteristic parameters are listed in Table 2, that is, the Al–O distance and the O-Al-O and Al-O–C bond angles. The Al–O distances of the $[hfip]^-$ and the $[hftb]^-$ anions are similar within the standard deviation, while those in the $[pftb]^-$ salt are slightly shorter. The most

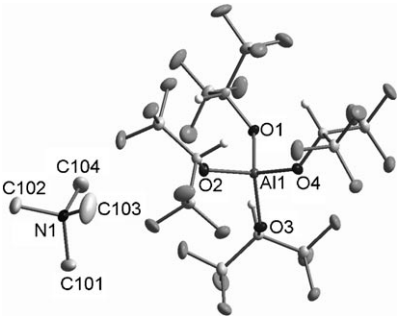

Figure 1. Section of the solid-state structure of **6** at 100 K. Thermal ellipsoids are drawn at the 25% probability level. In the asymmetric unit, there are two half cations, the other atoms have been symmetry-generated. H atoms at the methyl groups have been omitted for clarity. Selected distances and bond angles: d(Al1–O1) = 174.32(9), d(Al1–O2) = 174.44(10), d(Al1–O3) = 174.35(9), d(Al1–O4) = 173.67(19) pm, ∢(O4-Al1-O1) = 115.05(5), ∢(O4-Al1-O3) = 106.50(5), ∢(O1-Al1-O3) = 106.10(5), ∢(O4-Al1-O2) = 109.96(5), ∢(O1-Al1-O2) = 107.52(5), ∢(O3-Al1-O2) = 111.71(5)°.

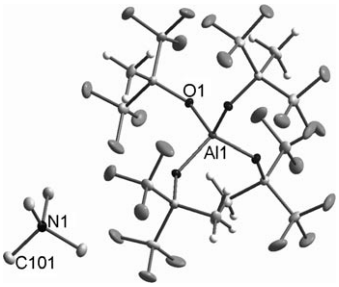

Figure 2. Section of the solid-state structure of **9** at 100 K. Thermal ellipsoids are drawn at the 25% probability level. In the asymmetric unit, there is one quarter cation and one quarter anion, the other atoms have been symmetry-generated. H atoms at the cation have been omitted for clarity. Selected distances and bond angles: d(Al1–O1) = 174.23(6) pm, ∢(O1-Al1-O1) = 109.5°.

significant difference between the perfluorinated and the other two anions are the Al-O-C bond angles. In the $[pftb]^-$ anion, the alkoxy moieties are larger and due to this sterical hindrance, the Al-O-C angle is greater.

From the data in Table 2 it may be concluded that the Al–O bond in the $[pftb]^-$ salts is slightly more stable; similar experiences have been made in experiments aiming at the synthesis of reactive cation salts with the $[hfip]^-$ and $[hftb]^-$ anions being less adequate for this purpose and therefore unsuitable to reach the extremely reactive species stabilized by the $[pftb]^-$ anion. A comment on the solid-date packing of all salts is deposited in the Supporting Information.

Establishment of the ion volumes of the $[Al(OR^F)_4]^-$ anions: Lattice energies derived from the molecular volumes of the ions in a salt ($V_m = V^+_{ion} + V^-_{ion}$) are the fundamental anchor point in the concept of volume-based thermodynamics (VBT) established first by Bartlett[47] and later in more detail by Glasser and Jenkins.[43,48] This concept allows thermodynamic predictions for condensed phases principally via formula unit volumes. In the case of ionic liquids, the knowledge of V_{ion} also allows to predict physical properties like melting points or dielectric constants.[49] The $[NR_4]^+$ salts of the $[Al(OR^F)_4]^-$ anions were chosen to establish precise V_{ion} of these anions, since in these salts, the anions have a nearly undisturbed environment and therefore, they are ideal candidates for such purpose. In Table 3, the values obtained from the solid-state structures of their $[NR_4]^+$ salts are compiled.

Table 3. Ion volumes V^-_{ion} of the $[Al(OR^F)_4]^-$ anions, based on the solid-state structures of their $[NR_4]^+$ salts at 100 K. All values are given in nm^3.

	$[hfip]^-$	$[hftb]^-$	$[pftb]^-$
$[NBu_4]^+[Al(OR^F)_4]^-$	–	0.6491 ± 0.009[c]	–
$[NEt_4]^+[Al(OR^F)_4]^-$	0.5727 ± 0.006	–	0.7361 ± 0.016[a]
$[NMe_4]^+[Al(OR^F)_4]^-$	0.5826 ± 0.015[b]	0.6664 ± 0.015[b]	–
V^-_{ion} (av.)	0.577	0.658	0.736

[a] $V^+_{ion}(NEt_4^+)$ from ref. [44]. [b] $V^+_{ion}(NMe_4^+)$ from ref. [44]. [c] $V^+_{ion}(NBu_4^+)$ from $[NBu_4]^+[IO_4]^-$[50] and $V^-_{ion}(IO_4^-)$ from ref. [44].

Vibrational spectra of the aluminates: The solid-state structures of the $[NR_4]^+$ salts (R = Me, Et, Bu) contain undisturbed anions with only very weak H-F contacts (see Supporting Information). If the cation is more coordinating (e.g., $Ag(CH_2Cl_2)^+$, Ag^+ or Li^+), the symmetry of the anion is lowered which leads to the splitting of some anion vibrational bands. In this Section, the different IR spectra are discussed—together with simulations from DFT calculations ((RI)BP86/SV(P) level, which usually slightly underestimate the vibrational frequencies). An explanation of the influence of the cations is given.

IR spectra of the $[pftb]^-$ salts: In Table 4 the vibrational frequencies of the $[pftb]^-$ anion in different compounds, that is, its $[NR_4]^+$, $[Ag(CH_2Cl_2)]$, Ag and Li salts, are listed, together with the simulated IR spectrum of the isolated anion.

Vibrational bands of the $[pftb]^-$ anion are found both in the MIR and the FIR region, the most characteristic absorptions are observed at 727 cm^{-1} (C–C, C–O) and 974 cm^{-1} (C–

Table 2. Characteristic structural information of the $[Al(OR^F)_4]^-$ anions in their tetraalkylammonium salts at 100 K. Distances are given in pm, bond angles are given in °.

	2	**5**	**6**	**7**	**9**
d(Al–O) [pm]	172.3(4)–174.2(4) av. 173.4	173.7(2)–175.0(3) av. 174.2	173.7(2)–174.4(1) av. 174.2	173.1(1)–174.2(1) av. 174.0	174.2(1)
∢(O-Al-O) [°]	107.2(1)–112.7(2) av. 109.5	102.9(1)–116.3(1) av. 109.5	106.5(1)–115.1(1) av. 109.5	105.9(1)–114.0(1) av. 109.5	109.5
∢(Al-O-C) [°]	144.9(4)-147.9(4) av. 146.8	124.5–133.7(2) av. 129.5	126.6(1)–136.3(1) av. 129.6	135.0(1)–141.6(1) av. 138.2	135.2(1)

C, C–F) as well as many strong bands in the range from 1100 to 1400 cm^{-1} (C–C, C–F). The comparison of the simulated spectra (Table 4) with those of $[NR_4]^+[pftb]^-$ shows that the anion has nearly S_4 symmetry in these compounds, because only the expected absorption maxima are observed. This is also in good agreement with the solid-state structure of $[NEt_4]^+[pftb]^-$ ***2*** determined by X-ray (see above).

Table 4. Calculated (RI-BP86/SV(P)) and experimental vibrational (IR and Raman) frequencies [cm^{-1}] of the $[pftb]^-$ anion **1**–**3**, $[Ag(CH_2Cl_2)][pftb]$, Ag[pftb] and Li[pftb].

$[pftb]^-$	**1**		**2**		**3**		$[Ag(CH_2Cl_2)][pftb]$	Ag[pftb]	Li[pftb]		Assignment
calcd	IR exptl	Raman exptl	IR exptl	Raman exptl	IR exptl	Raman exptl	IR exptl	IR exptl	IR exptl	Raman exptl	
189 (w)	227 (w)	233 (w)	228 (w)	234 (w)	–	235 (w)	–	–	–	234 (mw)	–
274 (w)	303 (w)	291 (w)	285 (mw)	289 (w)	289 (w)	289 (w)	288 (w)	290 (w)	289 (w)	297 (w)	C–C
301 (w)	315 (m)	322 (ms)	316 (m)	323 (ms)	316 (w)	322 (s)	316 (m)	319 (m)	–	326 (w)	C–C, Al–O
319 (w)	–	–	331 (w)	–	–	–	332 (w)	332 (w)	326 (w)	327 (m)	C–C, C–F, Al–O
352 (w)	367 (w)	369 (w)	367 (mw)	368 (w)	–	368 (m)	367 (w)	–	369 (w)	363 (w)	C–C, C–F, Al–O
364 (w)	382 (w)	–	377 (mw)	–	–	–	387 (mw)	391 (mw)	–	390 (w)	C–C, C–O
421 +436 (mw)	448 (ms)	–	446 (ms)	–	449 (m)	453 (ms)	443 (m)	435 (m)	–	–	C–C, C–O
–	–	–	–	–	–	–	468 (mw)	468 (m)	464 (m)	–	–
520 (mw)	536 (m)	538 (mw)	537 (m)	538 (w)	536 (m)	538 (mw)	537 (mw)	538 (ms)	539 (m)	539 (mw)	C–C, C–O
–	–	–	–	–	–	–	–	553 (mw)	546 (mw)	–	–
547 (mw)	559 (mw)	561 (w)	562 (mw)	563 (w)	560 (mw)	562 (mw)	561 (mw)	567 (mw)	562 (mw)	–	Al–O, C–C
556 (w)	573 (w)	572 (w)	571 (w)	–	571 (w)	572 (mw)	572 (mw)	575 (mw)	572 + 582 (m)	573 (mw)	Al–O, C–C
–	–	–	–	–	–	–	–	694 (w)	–	–	–
708 (m)	726 (ms)	–	727 (s)	–	725 (ms)		727 (ms)	727 (s)	726 (s)	730 (s)	C–C, C–O
–	–	744 (ms)	–	747 (ms)	–	747 (s)	–	743 (m)	740 (ms)	745 (s)	–
735 (w)	755 (w)	–	756 (mw)	–	756 (mw)	–	754 (w)	759 (w)	756 + 760 (m)	–	C–C, C–O
–	–	799 (ms)	–	798 (s)	–	794 (s)	796 (w)	796 (mw)	798 (m)	801 (w)	–
816 (w)	830 (m)	–	833 (m)	834 (w)	831 (m)	832 (w)	833 (mw)	827 (w)	844 (ms)	843 (w)	Al–O, C–C
825 (w)	–	–	–	–	–	–	–	862 (mw)	863 (ms)	–	Al–O, C–C
–	–	–	–	–	947 (sh)	–	–	–	936 (ms)	–	–
–	–	–	–	–	967 (sh)	–	964 (s)	–	964 (vs)	–	–
960 (s)	975 (vs)	975 (mw)	973 (s)	978 (mw)	976 (s)	976 (mw)	974 (ms)	974 (vs)	976 (vs)	978 (w)	C–C, C–F
1110 (w)	–	1133 (mw)	–	1139 (mw)		1135 (mw)	–	–	–	1113 (w)	C–C, C–F
1134 (w)	1176 (ms)	1173 (mw)	–	1173 (mw)	1163 (s)	–	1182 (m)	1182 (m)	1184 (ms)	1171 (w)	C–C, C–F
1218 (vs)	1223 (vs)	–	1217 (vs)	–		–	1224 (vs)	1218 (vs)	1225 (vs)	1214 (mw)	C–C, C–F
1230 (vs)	1236 (vs)	1237 (mw)	1240 (s)	1235 (mw)	1237 (vs)	1239 (mw)	1245 (vs)	1245 (vs)	1243 (s)	1250 (mw)	C–C, C–F
1260 (vs)	–	–	1254 (s)	–	–	–	1256 (s)	1259 (vs)	–	–	C–C, C–F
–	1274 (s)	1276 (mw)	1274 (vs)	1274 (mw)	1271 (vs)	1272 (mw)	–	–	1270 (s)	1281 (mw)	C–C, C–F
–	1299 (s)	–	1298 (s)	1300 (m)	1296 (s)	1307 (w)	1299 (ms)	1301 (s)	1297 (s)	–	C–C, C–F
1344 (vs)	1349 (ms)	1353 (w)	1353 (ms)	–	1351 (ms)	1352 (w)	1355 (mw)	1354 (m)	1353 (ms)	1337 (mw)	C–C, C–F

In the case of the $[Ag(CH_2Cl_2)]^+$ salt, splitting occurs for the bands at 974 cm^{-1} ($\rightarrow$ 964 and 974 cm^{-1}) and at 447 cm^{-1} ($\rightarrow$ 443 and 468 cm^{-1}). If $[Ag(CH_2Cl_2)][pftb]$ is dried in high vacuum (about 10^{-3} mbar) for two to four days, the coordinated CH_2Cl_2 molecule can be removed. As shown in Table 4, the IR spectra split further: Without the CH_2Cl_2 ligand, some new bands appear (at 553, 694, 743 and 862 cm^{-1}). In both silver salts the silver atom is supposed to be coordinated to the $[pftb]^-$ anion. Therefore, the symmetry is reduced, which leads to band splitting in the vibrational spectrum. Although the solid state structure of $Ag(CH_2Cl_2)[pftb]$ is yet unknown, it is very likely that—in analogy to the corresponding silver salts of $[hfip]^-$ and $[hftb]^-$ as well as in $[Ag(C_6H_4(CF_3)_2)][pftb]$[37]—the oxygen atoms are involved in this coordination. According to quantum mechanical calculations, the oxygen atoms are also the most basic parts of the $[pftb]^-$ anion (partial charge: −0.24),[7,15] and their polarizability is higher (0.802 instead of 0.557 for F).[51] In Ag[pftb], the symmetry is even more lowered due to stronger coordination. This causes the increased splitting of more anion bands. The same holds for the Li salt, but in this case, the splitting is even more distinct: between 539 and 582 cm^{-1} five signals are observed, next to the band at 760 cm^{-1}, a second one arises at 756 cm^{-1}, and the band at 964/976 cm^{-1} shows a broad shoulder. This is in line with the small size and the high charge density of the Li cation, which allows a strong interaction with the lone pairs of the oxygen atoms of the anion.

In all salts of the $[pftb]^-$ anion investigated in this study, the broader bands of the CF_3 groups (between 1100 and 1400 cm^{-1}) remain nearly unchanged upon anion coordination.

IR spectra of the [hfip]⁻ and [hftb]⁻ salts: For anions $[hfip]^-$ and $[hftb]^-$, characteristic vibrational excitations are also observed (Tables 5 and 6), which can also be used to distinguish between the different anions: in the case of the $[hftb]^-$ anion, the intense C–C/C–O and the C–C/C–F modes are found at 736 and 995 cm^{-1}, while for $[hfip]^-$ salts, they are found at around 730 and 1012 cm^{-1} (cf. 727 and 974 cm^{-1} for $[pftb]^-$). In both hydrogen-containing anions, C–H vibrations were found: at 1375, 2715 (only in the Raman spectra) and 2950 cm^{-1} for $[hftb]^-$ and at around 1455 and 2960 cm^{-1} for $[hfip]^-$. For the $[hftb]^-$ anion, also two weak bands above 3000 cm^{-1} were predicted by quantum chemical calculations, but in the case of the alkylammonium salts, these absorptions are covered by the bands of the cations, and in the Ag^+ and Li^+ salt, they are most probably too weak to be seen.

The influence of the anion–cation interactions on the vibrational spectra can also be seen for the $[hftb]^-$ and the $[hfip]^-$ anions: In the case of the $[hfip]^-$ anion, the most affected bands are those between 700 and 900 cm^{-1}: while for the NR_4^+ salts, only three bands are found in the IR and Raman spectra—as expected from the simulated spectrum of the anion—one observes splitting in the Ag^+ and Li^+ salt due to lowered symmetry, which leads to up to six bands (see arrows in Figure 3). The vibrations of the CF_3 moieties remain, like those in the $[pftb]^-$ salts, unchanged upon coordination. A comparison of our materials with previously reported ionic liquids containing the $[hfip]^-$ anion[41] are also in very good agreement.

Similar observations are also made for the $[hftb]^-$ anion. The Al–O, C–C and C–O vibrations are strongly dependent on the coordination ability of the countercation. The strong coordination to the Li^+ and Ag^+ in these salts also lowers the anion symmetry, and again, this can be seen from the vibrational spectra. The NR_4^+ salts have four absorptions between 730 and 1000 cm^{-1}, whereas in the case of Li^+, six different bands appear. Also for this anion, the bands of the CF_3 groups are (almost) not affected by coordination.

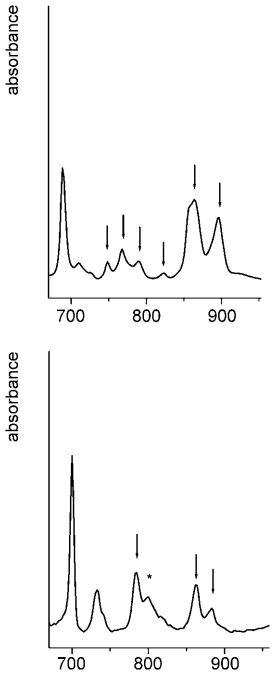

Figure 3. Comparison of sections of the IR spectra of Li[hfip] (top) and **4** (bottom). Bands marked with asterisks are assigned to the cation.

All these findings are also in very good agreement with the solid-state structures, in which nearly ideal symmetric anion environments have been found for their NR_4^+ salts.

Conductivity measurements: Tetraalkylammonium salts are often applied in electrochemical measurements, where they serve as supporting electrolytes in polar organic solvents such as CH_3CN. In solvents with very low polarity (e.g., in CH_2Cl_2 or even $HCCl_3$), the commonly used $[NR_4]^+[PF_6]^-$ and $[NR_4]^+[BF_4]^-$ electrolytes solubilize the electrochemically produced (multiply) charged cations only insufficient and tend to form insoluble layers on the electrode preventing the measurement. Moreover many higher charged cations that are generated in situ in the electrochemical cell are too reactive for those counterions and decompose the traditional $[PF_6]^-$ anion. Due to their superior solubilization properties and increased stability, large and weakly coordinating anions like $[B(C_6F_5)_4]^-$ considerably improve the performance in low dielectric solvents.[8–12] Using the difficult to prepare very lipophilic $[B_{11}CMe_{12}]^-$ anion,[13] even cyclovoltammetric measurements in benzene may be performed.[14] Another alternative to circumvent the solvent problem are tetralkylammonium salts with long alkyl chains which were used in ultramicroelectrode experiments without any supporting electrolyte.[41c]

Since the $[Al(OR^F)_4]^-$ anions are chemically rather robust and large, their electrochemical performance both with respect to solubility as well as conductivity in weakly polar solvents was tested. In Table 7, the molar conductivities of

Table 5. Calculated (RI-BP86/SV(P)) and experimental vibrational (IR and Raman) frequencies [cm^{-1}] of the $[hfip]^-$ anion in its Ag^+, Li^+, $[NBu_4]^+$, $[NEt_4]^+$ and $[NMe_4]^+$ salts.

$[hfip]^-$	**4**		**5**		**6**		Ag[hfip]	Li[hfip]		Assign-
calcd	IR exptl	Raman exptl	IR exptl	Raman exptl	IR exptl	Raman exptl	IR exptl	IR exptl	Raman exptl	ment
289 (w)	–	298 (w)	302 (w)	299 (w)	–	298 (w)	–	–	301 (w)	C–C, Al–O
–	–	–	–	–	–	–	–	320 (mw)	–	–
–	328 (w)	333 (mw)	330 (w)	331 (mw)	–	331 (mw)	332 (w)	–	333 (mw)	–
370 (mw)	377 (w)	369 (w)	367 (w)	357 (w)	–	–	–	379 (mw)	364 (mw)	C–C, C–F, Al–O
448 (w)	445 (mw)	–	438 (mw)	417 (mw)	444 (w)	–	421 (mw)	427 (mw)	450 (w)	C–C, C–O
487 (w)	–	–	–	–	–	–	463 (w)	470 (w)	485 (mw)	C–C, C–O
514 (w)	524 (mw)	526 (w)	521 (w)	524 (w)	522 (w)	525 (w)	523 (mw)	521 (mw)	527 (w)	C–C, C–O
–	536 (w)	537 (w)	–	536 (w)	–	537 (w)	537 (w)	537 (w)	539 (w)	–
547 (w)	567 (w)	569 (w)	570 (w)	566 (w)	570 (w)	571 (w)	563 (w)	563 (w)	556 (w)	C–C, Al–O
–	–	–	–	–	–	–	578 (w)	577 (w)	576 (w)	–
607 (mw)	597 (w)	600 (w)	–	–	–	–	–	–	–	C–C, Al–O
–	–	–	–	–	–	–	669 (w)	–	–	–
679 (m)	685 (m)	–	684 (m)	–	685 (m)	–	688 (m)	689 (ms)	–	C–C, Al–O
–	–	697 (w)	–	696(w)	–	698 (m)	–	–	692 (w)	–
–	–	–	–	–	–	–	---	–	708 (w)	–
721 (m)	–	729 (w)	727 (mw)	–	–	729 (w)	727 (w)	–	733 (w)	C–C, C–O
754 (m)	–	–	–		–	–	–	748 (w)	752 (mw)	C–C, C–O
–	–	763 (mw)	–	762 (mw)	777 (w)	765 (m)	760 (mw)	767 (w)	769 (m)	–
–	–	–	–	–	–	–	780 (mw)	–	–	–
–	791 (w)	–	783 (w)	–	–	–	793 (w)	790 (w)	829 (w)	–
–	–	–	–	–	–	–	–	828 (w)	–	–
874 (m)	855 (w)	860 (m)	854 (w)	857 (m)	858 (m)	853 (m)	859 (m)	864 (m)	858 (ms)	C–C, Al–O
–	888 (mw)	884 (w)	890 (mw)	891 (w)	891 (m)	893 (w)	895 (m)	896 (m)	898 (w)	–
–	–	910 (w)	–	905 (w)	–	–	–	–	–	–
–	–	930 (w)	–	–	–	933 (w)	---	–	–	–
1012 (ms)	–	1053 (w)	–	–	–	–	–	–	–	C–C, C–F
–	–	1068 (w)	–	1069 (w)	–	–	–	–	–	–
1033 (s)	1100 (m)	–	1096 (m)		1096 (m)	–	1091 (vs)	1102 (s)	1098 (mw)	C–C, C–F
–	–	1112 (mw)	–	1117 (mw)	–	1117 (mw)	–	–	–	–
1126 (vs)	–	1133 (mw)	–	–	–	–	1140 (s)	1136 (vs)	1133 (mw)	C–C, C–F
1147 (s)	–	1155 (mw)	–	–	1152 (m)	–	–	–	–	C–C, C–F
1174 (s)	1180 (vs)	1179 (w)	1169 (vs)	1187 (w)	1179 (vs)	1190 (w)	1187 (vs)	1188 (vs)	–	C–C, C–F
1195 (vs)	–	–	1207 (s)	1209 (w)	–	–	1216 (vs)	–	1204 (mw)	C–C, C–F
1225 (s)	1252 (vs)	–	–	–	–	–	1228 (vs)	1237 (vs)	1242 (mw)	C–C, C–F
–	–	–	–	–	–	1266 (w)	1259 (vs)	–	1266 (w)	
1294 (ms)	1288 (s)	1295 (mw)	1288 (s)	1300 (mw)	1294 (s)	1298 (w)	1288 (s)	1293 (s)	1297 (w)	C–C, C–F
1330 (s)	–	1324 (w)	–	–	–	–	–	–	–	C–C, C–F, C–H
–	1375 (ms)	1383 (w)	1377 (ms)	1379 (w)	1376 (ms)	1379 (ms)	1377 (ms)	1379 (ms)	1381 (w)	–
–	–	–	–	–	–	–	---	–	1390 (w)	–
–	–	2716 (w)	–	2715 (w)	–	2722 (w)	2726 (w)	–	2732 (w)	–
–	–	2757 (w)	–	2759 (w)	–	–	–	–	2759 (w)	–
2923 (m)	2975 (mw)	2944 (mw)	2951 (w)	2952 (mw)	–	2953 (m)	2951 (mw)	–	2958 (mw)	C–H

Table 6. Calculated (RI-BP86/SV(P)) and experimental vibrational (IR and Raman) frequencies (in cm^{-1}) of the $[hftb]^-$ anion in its Ag^+, Li^+, $[NBu_4]^+$, $[NEt_4]^+$ and $[NMe_4]^+$ salts.

$[hftb]^-$	**7**		**8**		**9**		Ag[hftb]	Li[hftb]		Assign-
calc.	IR exptl	Raman exptl	IR exptl	Raman exptl	IR exptl	Raman exptl	IR exptl	IR exptl	Raman exptl	ment
316 (w)	–	295 (w)	–	294 (w)	–	295 (mw)	–	–	296 (mw)	C–C, Al–O
367 (w)	327 (w)	337 (w)	–	337 (w)	–	337 (mw)	–	–	337 (w)	C–C, C–F, Al–O
409 (w)	372 (w)	366 (w)	370 (w)	369 (mw)	368 (w)	370 (mw)	371 (w)	368 (w)	370 (m)	C–C, C–O
–	–	–	–	–	–	388 (mw)	392 (w)	396 (mw)	394 (m)	–
427 (mw)	437 (w)	–	–	–	440 (w)	–	439 (mw)	443 (w)	446 (w)	C–C, C–O
–	–	–	–	–	–	–	455 (w)	–	–	–
487 (w)	522 (mw)	517 (w)	522 (mw)	517 (w)	512 (w)	518 (w)	518 (w)	512 (w)	514 (w)	C–C, C–O
525 (w)	–	534 (w)	534 (w)	535 (w)	–	536 (w)	535 (m)	534 (mw)	535 (w)	C–C, C–O
547 (w)	566 (w)	567 (w)	567 (w)	568 (w)	569 (w)	567 (w)	572 (m)	572 (w)	574 (w)	C–C, Al–O
595 (w)	622 (w)	622 (m)	623 (w)	622 (m)	622 (m)	622 (m)	621 (m)	–	622 (m)	C–C, Al–O
–	–	–	–	–	–	–	632 (m)	633 (w)	–	–
–	–	–	–	–	–	–	–	–	676 (w)	–
682 (mw)	700 (mw)	699 (mw)	700 (mw)	698 (mw)	700 (ms)	699 (mw)	702 (ms)	702 (ms)	701 (w)	C–C, Al–O, C–O
709 (mw)	736 (mw)	735 (mw)	733 (mw)	735 (mw)	735 (w)	741 (mw)	739 (m)	739 (w)	742 (w)	C–C, C–O
763 (w)	784 (mw)	770 (s)	783 (mw)	770 (s)	774 (mw)	772 (s)	772 (m)	773 (w)	774 (s)	C–C, C–O
–	–	–	–	–	791 (mw)	–	791 (m)	794 (w)	–	–
–	–	–	–	–	–	–	800 (m)	–	–	–
838 (w)	863 (w)	–	865 (w)	867 (w)	864 (m)	866 (w)	867 (mw)	869 (mw)	870 (w)	C–C, Al–O
–		–	–		–	–	981 (mw)	981 (mw)	–	
994 (w)	995 (mw)	997 (w)	994 (mw)	998 (mw)	993 (ms)	994 (w)	998 (mw)	995 (mw)	997 (w)	C–C, C–F
–	–	1053 (w)	–	1069 (w)	–	–	–	–	1065 (w)	
1063 (s)	1077 (ms)	–	1078 (ms)	–	1080 (vs)	1082 (w)	1084 (vs)	1087 (vs)	1097 (w)	
1105 (s)	1112 (s)	–	1112 (s)	1117 (mw)	1115 (s)	1118 (w)	1118 (s)	1121 (s)	1121 (w)	C–C, C–F
1156 (s)	1177 (s)	1187 (w)	1178 (s)	1174 (w)	–	1167 (w)	1185 (s)	–	–	C–C, C–F
1177 (vs)										
1198 (s)										
1243 (s)	–	–	–	–	1183 (vs)	1202 (w)	1210 (vs)	1196 (vs)	1213 (w)	C–C, C–F
1255 (vs)	1233 (s)	1237 (mw)	1235 (s)	1242 (w)	1232 (s)	1235 (w)	1229 (vs)	1230 (vs)	1250 (w)	C–C, C–F
1306 (vs))	1307 (s)	1323 (w)	1308 (s)	1300 (w)	1307 (ms)	1319 (w)	1311 (s)	1311 (s)	1317 (w)	C–C, –F
1351 (m)	1384 (mw)	1387 (w)	1386 (s)	1395 (w)	1389 (w)	1390 (w)	–	1392 (mw)	1393 (w)	C–C, C–F
1432 (w)	1457 (w)	1453 (ms)	1462 (s)	1464 (ms)	1460 (w)	1456 (m)	1460 (mw)	1460 (mw)	1464 (m)	C–H
2975 (w)	2968 (mw)	–	–	2958 (m)	2963 (w)	2958 (m)	–	–	2901 (m)	C–H
3071 (w)	_[a]	_[a]	_[a]	_[a]	_[a]	_[a]	2962 (ms)	–	2965 (s)	C–H
3080 (w)	_[a]	_[a]	_[a]	_[a]	_[a]	_[a]	3012 (mw)	–	3017 (ms)	C–H

[a] Obscured by NR_4^+ cation bands.

the $[NBu_4]^+$ salts in four different solvents are listed, together with the values for $[NBu_4]^+[PF_6]^-$ examined in our laboratories. If compared to the widely used $[NBu_4]^+[PF_6]^-$, only the $[NBu_4]^+[hftb]^-$ salt **7** shows a higher molar solubility in CH_2Cl_2. The relatively high solubilities of $[NBu_4]^+[PF_6]^-$ are caused by strong ion-pairing effects in this salt. The higher solubility of **7** ($>1\ mol\,L^{-1}$ in CH_2Cl_2) can best be explained by the influence of the CH_3 moieties, which

Table 7. Solubilities (c_{max} in mol L^{-1}), absolute (Λ_{abs} in μS cm^{-1}) and molar conductivities (Λ_m in S cm^2 mol^{-1}) of **1**, **4**, **7** and $[NBu_4]^+[PF_6]^-$ at 25 °C.

	CH_2Cl_2				$CHCl_3$				CH_3CN				C_6H_5F			
	c_{max}	c	Λ_{abs}	Λ_m	c_{max}	c	Λ_{abs}	Λ_m	c_{max}	c	Λ_{abs}	Λ_m	c_{max}	c	Λ_{abs}	Λ_m
1	0.04	0.01	357	41.5	< 0.01	–	–	–	0.03	0.01	954	110.9	0.06	0.01	77	9.0
		0.001	56	65.1		–	–	–		0.001	113	131.3		0.001	10	11.6
4	1.09	0.01	378	106.3	0.03	–	–	–	0.21	0.01	953	268.1	0.26	0.01	49	13.8
		0.001	60	168.8		–	–	–		0.001	135	380.0		0.001	6	16.7
7	0.27	0.01	325	96.9	0.39	0.01	18	5.4	0.08	0.01	1118	333.3	0.06	0.01	53	15.8
		0.001	53	158.0		0.001	2	6.0		0.001	128	381.6		0.001	7	20.9
$[NBu_4]^+[PF_6]^-$	0.59	0.01	155	6.0	1.17	0.01	6	0.2	0.43	0.01	1435	55.6	1.01	0.01	61	2.4

make this anion more lipophilic than the perfluorinated [pftb]$^-$.

The lipophilicity of the [hfip]$^-$ anion lies in between that of [pftb]$^-$ and [hftb]$^-$, which is also in good agreement with the solubility of its NBu_4 salt. The stronger tendency of $[PF_6]^-$ to form ion pairs can also be seen from the molar conductivities. Even though this anion is by far the smallest, the molar conductivities of its $[NBu_4]^+$ salt are always lower if compared to those of the fluorinated aluminates.

The electrochemical stability of the $[NBu_4]^+$ salts (i.e., their "electrochemical window" in various non-polar solvents) is included with Table 8.

Table 8. Electrochemical windows of **1**, **7** and $[NBu_4]^+[PF_6]^-$ in CH_2Cl_2, 1,2-$F_2C_6H_4$ and CH_3CN.[a]

Salt	Solvent	U_{min} [V]	U_{max} [V]
1	CH_2Cl_2	−2.3	2.2
	1,2-$F_2C_6H_4$	−2.2	2.1
	CH_3CN	−1.7	1.1
7	CH_2Cl_2	−2.3	2.1
	1,2-$F_2C_6H_4$	−2.2	2.1
	CH_3CN	−1.6	1.1
$[NBu_4]^+[PF_6]^-$	CH_2Cl_2	−1.6	1.7
	1,2-$F_2C_6H_4$	−2.2	2.1
	CH_3CN	−1.0	0.9

[a] All values referred to the ferrocenium/ferrocene redox couple (external calibration for each solvent). Cut-off for current density J: $\pm 7 \times 10^{-5}$ A cm^{-2}. Actual scans and reference scans are deposited in the Supporting Information.

From Table 8 follows that the electrochemical window in a given solvent may be enlarged by the use of the aluminate electrolytes by up to +0.5 and −0.7 V. This shows most drastically for CH_2Cl_2.

Mass spectrometry: From some of the $[NR_4]^+$ salts of the [pftb]$^-$, [hfip]$^-$ and [hftb]$^-$ anions, ESI mass spectra in CH_3CN have been recorded in order to investigate anion decomposition pathways and correlate them to observed/postulated decomposition pathways with extremely electrophilic cations. Under the relatively mild conditions of the electrospray ionization, all three anions remain intact (m/z 967, 695 and 751 for [pftb]$^-$, [hfip]$^-$ and [hftb]$^-$ anions respectively), but upon collision experiments, in all three cases, the major decomposition product is the $[F\text{-}Al(OR^F)_3]^-$ anion. The mechanism of this degradation is sketched in Scheme 1. For the [pftb]$^-$ anion, this decomposition route has also been observed in the condensed phase, that is, during the formation of the $[(R^FO)_3Al\text{-}F\text{-}Al(OR^F)_3]^-$ anion.[52]

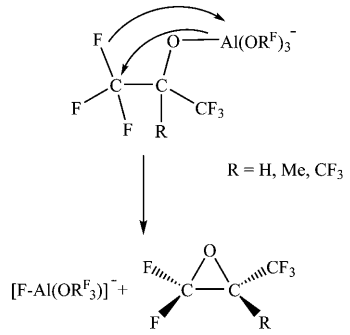

Scheme 1. Decomposition of the $[Al(OR^F)_4]^-$ anions in the mass spectrometer.

Conclusion

The tetraalkylammonium salts of the fluorinated alkoxyaluminates are easily accessible in large scale with good yields by simple metathesis reactions of their lithium salts with $[NR_4]Br$ (R = Me, Et, Bu) in water or Et_2O/CH_2Cl_2. The $[NR_4]^+[A]^-$ salts (A = anion) provide nearly undisturbed anion environments, which allowed to determine reliable values for ion volumes of the anions and made it possible to investigate their vibrational spectra in comparison to those of their Li^+ and Ag^+ salts, in which some of the bands are split because the anions are strongly coordinated by the cations.

The high solubility of $[NR_4]^+[A]^-$ salts in non-polar solvents like CH_2Cl_2 or $CHCl_3$ (up to 1.09 M for $[NBu_4]^+$[hftb]$^-$ (**7**) in CH_2Cl_2 and 0.41 M for **4** in $CHCl_3$) as well as their large electrochemical window (Table 8) makes them ideal supporting electrolytes in electrochemical processes, such as cyclic voltammetry. Compound **7** may even be suitable for toluene solution. In their electrochemical properties, they resemble the $[NR_4]^+$ salts of the $[B(C_6F_5)_4]^-$ anion,[11,12] but the synthesis of this fluorinated borate is much more complicated and also more expensive. They provide also a good alternative to the widely used $[PF_6]^-$ salts in non-polar media. In contrast to $[NBu_4]^+[PF_6]^-$, they even show a small conductivity in toluene ($\varepsilon_r = 2.2$), a solvent in which the

most tetraalkylammonium salts are insoluble or only dissolve as tight ion-pairs.

Experimental Section

Some reactions were carried out inside a glovebox under Ar atmosphere (<1 ppm O_2 and H_2O). All solvents were dried and distilled according to reported procedures and were anhydrous to a level of about 3 to 5 ppm H_2O (Karl Fischer Titration). IR measurements were performed on am ATR Nicolet (MAGNA IR 760) equipped with diamond ATR cell, no ATR correction was employed for the spectra. FT-Raman measurements were performed on a Bruker Vertex 70 spectrometer with a Ram II module equipped with a highly sensitive Ge detector. NMR measurements were performed on a Bruker 400 MHz Avance NMR. Electron spray ionization mass spectrometry (ESI-MS) was performed on a Thermo-LCQ-Advantage spectrometer using CH_3CN as carrier. DSC measurements were performed on a Setaram Instrument (DSC 131, KEP Technologies) using Al crucibles (30 μL). Complimentary melting point determinations were carried out on a standard melting point device (Lab devices, 50–60 cycles, 200 Watt). The melting points given were the average of at least two determinations of independent batches that differed by less than 4 °C. All were melting points and no glass transitions (DSC). Electrochemistry: working electrode: glass-carbon-electrode (3 mm diam.) reference electrode: Ag wire counter electrode: Au wire scan rate: 20 mV s^{-1}. The CV curves were recorded with Autolab PGSTAT 30 (Eco Chemie B.V., Utrecht, The Netherlands). Conductivity measurement: Metrohm 712; measurements done inside a glove box.

Computational details: All calculations have been performed with the program package TURBOMOLE 5.8[53] using the RI-BP86 method and the SV(P) basis set.[54,55] Vibrational excitations have been calculated with the module AOFORCE[56] included in TURBOMOLE; the spectra were then obtained by a superposition of Gauss-type functions.

General method for the synthesis of $[NR_4]^+[pftb]^-$ (R=Bu 1, Et 2, Me 3): 1 equiv Li[pftb] and 1 equiv $[NR_4]Br$ were weighed in two different beakers and were dissolved in a mixture of dest. H_2O and acetone (85:15 v/v about 10–20 mL per 1 g Li[pftb]). The two solutions were mixed and stirred for a few minutes at room temperature. The reaction mixture was kept over night at a warm place (approx. 30 °C, for example, on top of a heating oven) so that the acetone part of the solvent was evaporated. The over night forming microcrystalline colorless precipitate was filtered over a Buchner frit and washed first with water (until no Br^- was present, testing with Ag^+) and then two times with hexane (approx. 10 mL per 1 g Li[pftb]). The white, crystalline product was dried over night at 60 °C in an oven.

All IR and Raman spectra are included with the Tables in the main text.

$[NBu_4]^+[pftb]^-$ (1): Isolated yield: 11.000 g (95.7 %); m.p. (DSC): 198 °C; ^{1}H NMR (400.0 MHz, CD_2Cl_2, 300 K): δ = 1.00 (t, J = 7 Hz, 3 H, CH_3), 1.60 (m, 2 H, CH_2), 1.57 (m, 2 H, CH_2), 3.03 ppm (m, 3 H, N(CH_2)); ^{13}C{^{1}H} NMR (100.6 MHz, CD_2Cl_2, 300 K): δ = 13.9 (s), 20.2 (s), 24.5 (s), 49.8 (s), 79 (m), 122.0 ppm (q, J = 293 Hz); ^{19}F NMR (376.5 MHz, CD_2Cl_2/CH_3CN, 300 K): δ = −75.8 ppm; ^{27}Al NMR (104.3 MHz, CD_2Cl_2, 300 K): δ = 31.9 ppm (s, $\omega_{1/2}$ = 9 Hz); elemental analysis calcd (%) for: C 31.55, H 3.08, N 1.10; found: C 31.78, H 3.00, N 1.16 (1.10).

$[NEt_4]^+[pftb]^-$ (2): Isolated yield: 10.700 g (93.0 %); m.p. (DSC): > 300 °C; ^{1}H NMR (400.0 MHz, CD_2Cl_2/CH_3CN, 300 K): δ = 1.27 (tt, 3 H, CH_3), 3.20 ppm (m, 2 H, N(CH_2)); ^{13} NMR (100.6 MHz, CD_2Cl_2, 300 K): δ = 8.8 (s), 50.9 (s), 79 (m), 122.0 ppm (q, J = 293.5 Hz); ^{13}C {^{1}H} NMR (63 MHz, [D_6]acetone, 300 K): δ = 7.5 (s), 52.9 (s), 122.0 ppm (q, J = 293.5 Hz); ^{19}F NMR (376.5 MHz, CD_2Cl_2/CH_3CN, 300 K): δ = −75.8 ppm (s); ^{27}Al NMR (104.3 MHz, CD_2Cl_2/CH_3CN, 300 K): δ = 31.9 ppm (s, $\omega_{1/2}$ = 12 Hz); ESI-MS(−): m/z: 967.2 $[Al(OC(CF_3)_3)_4)]^-$; MS/MS: m/z: 967.1 $[Al(OC(CF_3)_3)_4)]^-$, 751.1 $[F–Al(OC(CF_3)_3)_3]^-$; elemental analysis calcd (%) for: C 25.96, H 1.81, N 1.20; found; C 26.27, H 1.84, N 1.28.

$[NMe_4]^+[pftb]^-$ (3): Isolated yield: 4.790 g (95.8 %); m.p. (DSC): > 300 °C; ^{1}H NMR (400.0 MHz, CD_2Cl_2/CD_3CN, 300 K): δ = 3.03 ppm (s); ^{13}C{^{1}H} NMR (100.6 MHz, CD_2Cl_2/CD_3CN, 300 K): δ = 55.6 (s), 80 (m), 122.0 ppm (q, J = 293 Hz); ^{19}F NMR (376.5 MHz, CD_2Cl_2/CD_3CN, 300 K): δ = −75.7 ppm (s); ^{27}Al NMR (104.3 MHz, CD_2Cl_2/CD_3CN, 300 K): δ = 35 ppm (s, $\omega_{1/2}$ = 12 Hz); elemental analysis calcd (%) for C 23.48, H 1.14, N 1.27; found: C 23.07, H 1.66, N 1.35.

General method for the synthesis of $[NR_4]^+[hfip]^-$ (R=Bu 4, Et 5, Me 6) and $[NR_4]^+[hftb]^-$ (R=Bu 7, Et 8, Me 9): 1 equiv Li[A] and 1 equiv $[NBu_4]Br$ were weighed together into a Schlenk vessel. About 30 mL diethyl ether were added per 1 g Li[A] and the reaction mixture was stirred at room temperature (for R = Bu: 30 minutes, for R = Et: 1 h, for R = Me: over night) before the solvent was removed by vacuum distillation. After the addition of CH_2Cl_2 (approx. 5–10 mL per 1 g Li[A]) the mixture was filtered over a Al_2O_3 column. The solution was then concentrated until the product recrystallized at 2 °C. All IR and Raman data are in the Tables in the main text.

$[NBu_4]^+[hfip]^-$ (4): Isolated yield: 3.927 g (78.5 %); m.p. (DSC): 40 °C (190 °C: decomposition); ^{1}H NMR (400.0 MHz, CD_2Cl_2, 300 K): δ = 1.02 (t, J = 7 Hz, 3 H, CH_3), 1.42 (m, 2 H, CH_2), 1.59 (m, 2 H, CH_2), 3.07 (m, N-(CH_2)), 4.51 ppm (m, 1 H, CH); ^{13}C{^{1}H} NMR (100.6 MHz, CD_2Cl_2, 300 K): δ = 13.7 (s), 20.4 (s), 24.4 (s), 59.8 (s), 71.7 (sep), 123.8 ppm (q, J = 285 Hz); ^{19}F NMR (376.5 MHz, CD_2Cl_2, 300 K): δ = −77.3 ppm (d, J = 5.7 Hz); ^{27}Al NMR (104.3 MHz, CD_2Cl_2, 300 K): δ = 57.8 ppm (s, $\omega_{1/2}$ = 73 Hz); elemental analysis calcd (%) for: C 38.43, H 5.07, N 1.34; found: C 38.68, H 4.87, N 1.41.

$[NEt_4]^+[hfip]^-$ (5): Isolated yield: 3.533 g (70.7 %); m.p. (DSC): 56 °C; ^{1}H NMR (400.0 MHz, CD_2Cl_2, 300 K): δ = 1.27 (tt, 3 H, CH_3), 3.12 (m, 2 H, N(CH_2)), 4.50 ppm (m, 1 H, CH); ^{13}C{^{1}H} NMR (100.6 MHz, CD_2Cl_2, 300 K): δ = 7.7 (s), 53.3 (s), 72.0 (m), 123.2 ppm (q, J = 285 Hz). ^{19}F NMR (376.5 MHz, CD_2Cl_2, 300 K): δ = −77.3 ppm (s); ^{27}Al NMR (104.3 MHz, CD_2Cl_2, 300 K): δ = 57.6 ppm (s, $\omega_{1/2}$ = 90 Hz); ESI-MS(−): m/z: 695.2 $[Al(OC(H)(CF_3)_2)_4)]^-$; MS/MS: m/z: 695.2 $[Al(OC(H)-(CF_3)_2)_4)]^-$, 547.2 $[FAl(OC(H)(CF_3)_2)_3]^-$; elemental analysis calcd (%) for: C 32.45, H 3.87, N 1.47; found: C 32.70, H 3.66, N 1.59.

$[NMe_4]^+[hfip]^-$ (6): Isolated yield: 3.154 g (71.6 %); m.p. (DSC): 43 °C; ^{1}H NMR (400.0 MHz, CD_2Cl_2/CD_3CN, 300 K): δ = 3.03 (s, 3 H, N(CH_3), 4.50 ppm (m, 1 H, CH); ^{13}C{^{1}H} NMR (100.6 MHz, CD_2Cl_2/CD_3CN, 300 K): δ = 55.8 (s),71.1 (sept), 126.1 ppm (q, J = 285 Hz); ^{19}F NMR (376.5 MHz, CD_2Cl_2/CD_3CN, 300 K): δ = −77.5 ppm (s); ^{27}Al NMR (104.3 MHz, CD_2Cl_2/CD_3CN, 300 K): δ = 57.5 ppm (s, $\omega_{1/2}$ = 95 Hz).

$[NBu_4]^+[hftb]^-$ (7): Isolated yield: 1.702 g (85.1 %); m.p. (DSC): 106 °C; ^{1}H NMR (400.0 MHz, CD_2Cl_2, 300 K): δ = 1.00 (t, J = 7 Hz, 3 H, CH_3), 1.40 (m, 2 H, CH_2), 1.49 (s, 3 H, C(CH_3)), 1.57 (m, 2 H, CH_2), 3.04 ppm; ^{13}C{^{1}H} NMR (100.6 MHz, CD_2Cl_2, 300 K): δ = 13.7 (s), 18.1 (s), 20.1 (s), 24.4 (s), 59.6 (s),75.9 (m), 125.3 ppm (q, J = 289 Hz); ^{19}F NMR (376.5 MHz, CD_2Cl_2, 300 K): δ = −79.5 ppm (s); ^{27}Al NMR (104.3 MHz, CD_2Cl_2, 300 K): δ = 46.9 ppm (s, $\omega_{1/2}$ = 9 Hz); ESI-MS(−): m/z: 751.3 $[Al(OC(CH_3)(CF_3)_2)_4)]^-$; MS/MS: m/z: 751.2 $[Al(OC(CH_3)(CF_3)_2)_4)]^-$, 667.2 $[hftb–CH_3–CF_3]^-$, 589.3 $[FAl(OC(CH_3)(CF_3)_2)_3]^-$; elemental analysis calcd (%) for: C 29.18, H 2.92, N 1.63; found: C 29.10, H 2.93, N 1.70.

$[NEt_4]^+[hftb]^-$ (8): Isolated yield: 1.527 g (76.3 %); m.p. (DSC): 110 °C; ^{1}H NMR (400.0 MHz, CD_2Cl_2, 300 K): δ = 1.31 (tt, 3 H, CH_3), 1.48 (s, 3 H, C(CH_3)), 3.14 ppm (m, 2 H, N(CH_2)); ^{13}C{^{1}H} NMR (100.6 MHz, CD_2Cl_2, 300 K): δ = 7.9 (s), 18.3 (s), 53.4 (s), 77 (m), 125.0 ppm (q, J = 291 Hz); ^{19}F NMR (376.5 MHz, CD_2Cl_2, 300 K): δ = −79.9 ppm (s); ^{27}Al NMR (104.3 MHz, CD_2Cl_2, 300 K): δ = 46.8 ppm (s, $\omega_{1/2}$ = 7 Hz); elemental analysis calcd (%) for: C 35.19,H 4.48, N 1.40; C 35.87, H 4.30, N 1.49.

$[NMe_4]^+[hftb]^-$ (9): Isolated yield: 1.702 g (85.1 %); m.p. (DSC): 94 °C; ^{1}H NMR (400.0 MHz, CD_2Cl_2/CD_3CN, 300 K): δ = 1.42 (s, 3 H, C(CH_3)), 3.01 ppm (m, 3 H, N(CH_3)); ^{13}C{^{1}H} NMR (100.6 MHz, CD_2Cl_2/CD_3CN, 275 K): δ = 17.8 (s), 55.9 (s), 75.8 (m), 125.0 ppm (q, J = 289.0 Hz); ^{19}F NMR (376.5 MHz, CD_2Cl_2/CD_3CN, 300 K): δ = −79.8 ppm (s); ^{27}Al NMR (104.3 MHz, CD_2Cl_2/CD_3CN, 300 K): δ = 50.2 ppm (s, $\omega_{1/2}$ = 9 Hz).

Crystallographic data for compounds **2**, **5–7**, **9** are available in Table 9.

Table 9. Crystallographic details for **2** at 100 K, **5** at 100 K and 140 K, **6** at 100 K, **7** at 100 K and **9** at 100 K.

	2	**5** (100 K)	**5** (140 K)	**6**	**7**	**9**
crystal size [mm]	0.2×0.2×0.2	0.3×0.3×0.1	0.2×0.3×0.2	0.2×0.2×0.3	0.3×0.3×0.4	0.2×0.2×0.1
crystal system	monoclinic	monoclinic	monoclinic	monoclinic	monoclinic	tetragonal
space group	$P2_1/c$	$P2_1/c$	$P2_1/c$	$P2_1/c$	$P2_1/c$	$I\bar{4}$
a [pm]	1393.6(3)	926.00(19)	925.27(19)	1061.3(2)	1758.0(4)	1291.70(18)
b [pm]	1889.7(4)	1900.2(4)	1899.9(4)	1381.1(3)	1410.2(3)	1291.70(18)
c [pm]	1420.8(3)	1851.3(4)	1854.6(4)	1898.8(4)	1958.1(4)	9.3184(19)
α [°]	90	90	90	90	90	90
β [°]	91.43(3)	99.28(3)	99.17(3)	91.42(3)	115.41(3)	90
γ [°]	90	90	90	90	90	90
V [nm^3]	3.7405(13)	3.2149(11)	3.2186(11)	2.7822(10)	4.3848(15)	1.5548(4)
Z	4	4	4	4	4	2
ρ_{calcd} [Mg m^{-3}]	1.949	1.705	1.703	1.837	1.505	1.763
μ [mm^{-1}]	0.270	0.231	0.231	0.260	0.184	0.239
abs. correction	none	none	none	none	none	none
$F(000)$	2160	1648	1648	1520	2032	824
index range	$-h \le 16$	$-10 \le h \le 10$	$-11 \le h \le 8$	$-13 \le h \le 13$	$-20 \le h \le 20$	$-17 \le h \le 17$
	$-22 \le k \le 22$	$-22 \le k \le 22$	$-23 \le k \le 23$	$-17 \le k \le 17$	$-16 \le k \le 13$	$-17 \le k \le 17$
	$-16 \le l \le 16$	$-21 \le k \le 21$	$-22 \le l \le 18$	$-24 \le l \le 24$	$-21 \le l \le 23$	$-12 \le l \le 12$
max 2θ	49.42	49.42	51.92	54.60	49.42	57.80
T [K]	100(2)	100(2)	140(2)	100(2)	100(2)	100(2)
diffractometer type	Bruker Apex II	Bruker Apex II	Kuma CCD	Bruker Apex II	Bruker Apex II	Bruker Apex II
unique reflns. [$I > 2\sigma(I)$]	6241	5085	5968	6274	7225	2054
data/restraints/parameters	6241/42/672	5085/0/491	5968/0/527	6274/0/416	7225/0/560	2054/0/137
GOOF	1.660	1.049	1.024	1.036	1.064	1.040
final $R1$ [$I > 2\sigma(I)$]	0.1128	0.0731	0.0563	0.0378	0.0428	0.0244
final $wR2$	0.3314	0.1345	0.1419	0.0934	0.0849	0.0608
largest residual peak [e Å^{-3}]	0.877	0.446	0.372	0.821	0.542	0.215
largest residual hole [e Å^{-3}]	−0.845	−0.376	−0.424	−0.385	−0.323	−0.144

Acknowledgement

This work was supported by the Deutsche Forschungsgemeinschaft DFG (SPP 1191 and Normalverfahren), the Albert-Ludwigs Universität Freiburg, Germany, the Ecole Polytechnique Fédérale in Lausanne, Switzerland, as well as the Schweizer Nationalfonds SNF. We thank Dr. Carsten Vock (EPF Lausanne) for recording the ESI-MS und MS-MS spectra.

[1] N. J. Stone, D. A. Sweigart, A. M. Bond, *Organometallics* **1986**, *5*, 2553–2555.
[2] C. G. Zoski, D. A. Sweigart, N. J. Stone, P. H. Rieger, E. Mocellin, T. F. Mann, D. R. Mann, D. K. Gosser, M. M. Doeff, A. M. Bond, *J. Am. Chem. Soc.* **1988**, *110*, 2109–2116.
[3] J.-Y. Cheng, Y.-H. Chu, *Tetrahedron Lett.* **2006**, *47*, 1575–1579.
[4] Z. Fei, D. Kuang, D. Zhao, C. Klein, W. H. Ang, S. M. Zakeeruddin, M. Graetzel, P. J. Dyson, *Inorg. Chem.* **2006**, *45*, 10407–10409.
[5] W. Li, Y. Oyama, M. Matsui in *Battery with molten salt electrolyte and high voltage positive active material* (Toyota Technical Center USA, Inc., USA; Toyota Motor Company, Japan); Application, WO 2006026773, **2006**, 23 pp.
[6] H. Nishida, N. Takada, M. Yoshimura, T. Sonoda, H. Kobayashi, *Bull. Chem. Soc. Jap.* **1984**, *57*, 2600–2604.
[7] I. Krossing, I. Raabe, *Angew. Chem.* **2004**, *116*, 2116–2142; *Angew. Chem. Int. Ed.* **2004**, *43*, 2066–2090.
[8] P. G. Gassman, P. A. Deck, *Organometallics* **1994**, *13*, 1934–1939.
[9] P. G. Gassman, J. R. Sowa, Jr., M. G. Hill, K. R. Mann, *Organometallics* **1995**, *14*, 4879–4885.
[10] M. G. Hill, W. M. Lamanna, K. R. Mann, *Inorg. Chem.* **1991**, *30*, 4687–4690.
[11] F. Barriere, W. E. Geiger, *J. Am. Chem. Soc.* **2006**, *128*, 3980–3989.
[12] A. Nafady, T. T. Chin, W. E. Geiger, *Organometallics* **2006**, *25*, 1654–1663.
[13] B. T. King, B. C. Noll, A. J. McKinley, J. Michl, *J. Am. Chem. Soc.* **1996**, *118*, 10902–10903.
[14] L. Pospisil, B. T. King, J. Michl, *Electrochim. Acta* **1998**, *44*, 103–108.
[15] I. Krossing, I. Raabe, *Chem. Eur. J.* **2004**, *10*, 5017–5030.
[16] B. G. Nolan, S. Tsujioka, S. H. Strauss in *Fluorinated Materials for Energy Conversion* (Eds.: T. Nakajima, H. Groult), **2005**, pp. 195–221.
[17] S. Tsujioka, B. G. Nolan, H. Takase, B. P. Fauber, S. H. Strauss, *J. Electrochem. Soc.* **2004**, *151*, A1418–A1423.
[18] H. Tokuda, S.-i. Tabata, S. Seki, M. Watanabe, *Kobunshi Ronbunshu* **2006**, *63*, 1–10.
[19] M. Watanabe, S. Tsujioka in *Room-temperature molten compounds having ate complexes and showing high ionic conductivity at room temperature for battery electrolytes* (Yokohama TLO Company, Ltd., Japan; Central Glass Co., Ltd.). Application, JP 2004067554, **2004**, 12 pp.
[20] H. Tokuda, M. Watanabe, *Electrochim. Acta* **2003**, *48*, 2085–2091.
[21] I. Krossing, A. Bihlmeier, I. Raabe, N. Trapp, *Angew. Chem.* **2003**, *115*, 1569–1572; *Angew. Chem. Int. Ed.* **2003**, *42*, 1531–1534.
[22] I. Raabe, D. Himmel, S. Müller, N. Trapp, M. Kaupp, I. Krossing, *Dalton Trans.* **2008**, 946–956.
[23] a) M. Gonsior, I. Krossing, L. Müller, I. Raabe, M. Jansen, L. Van Wüllen, *Chem. Eur. J.* **2002**, *8*, 4475–4492; b) G. Santiso-Quiñones, A. Reisinger, J. Slattery, I. Krossing, *Chem. Commun.* **2007**, 5046–5048.
[24] M. Gonsior, L. Müller, I. Krossing, *Chem. Eur. J.* **2006**, *12*, 5815–5822.
[25] M. Gonsior, I. Krossing, *Dalton Trans.* **2005**, 1203–1213.
[26] I. Krossing, *J. Chem. Soc. Dalton Trans.* **2002**, 500–512.
[27] M. Gonsior, I. Krossing, E. Matern, *Chem. Eur. J.* **2006**, *12*, 1703–1714.
[28] M. Gonsior, I. Krossing, E. Matern, *Chem. Eur. J.* **2006**, *12*, 1986–1996.
[29] I. Krossing, L. Van Wüllen, *Chem. Eur. J.* **2002**, *8*, 700–711.
[30] I. Krossing, *J. Am. Chem. Soc.* **2001**, *123*, 4603–4604.
[31] A. Adolf, M. Gonsior, I. Krossing, *J. Am. Chem. Soc.* **2002**, *124*, 7111–7116.

[32] I. Raabe, S. Antonijevic, I. Krossing, *Chem. Eur. J.* **2007**, *13*, 7510–7522.
[33] T. S. Cameron, A. Decken, I. Dionne, M. Fang, I. Krossing, J. Passmore, *Chem. Eur. J.* **2002**, *8*, 3386–3401.
[34] M. Gonsior, S. Antonijevic, I. Krossing, *Chem. Eur. J.* **2006**, *12*, 1997–2008.
[35] A. Reisinger, F. Breher, D. V. Deubel, I. Krossing, unpublished results.
[36] I. Krossing, A. Reisinger, *Angew. Chem.* **2003**, *115*, 5903–5906; *Angew. Chem. Int. Ed.* **2003**, *42*, 5725–5728.
[37] a) I. Krossing, *Chem. Eur. J.* **2001**, *7*, 490–502. b) S. M. Ivanova, B. G. Nolan, Y. Kobayashi, S. M. Miller, O. P. Anderson, S. H. Strauss, *Chem. Eur. J.* **2001**. *7*, 503–510.
[38] I. Krossing, H. Brands, R. Feuerhake, S. Koenig, *J. Fluorine Chem.* **2001**, *112*, 83–90.
[39] I. Krossing, A. Reisinger, *Eur. J. Inorg. Chem.* **2005**, 1979–1989.
[40] I. Krossing, A. Reisinger, *Coord. Chem. Rev.* **2006**, *250*, 2721–2744.
[41] a) T. Timofte, S. Pitula, A.-V. Mudring, *Inorg. Chem.* **2007**, *46*, 10938–10940. b) T. Timoffe, A.-V. Mudring, *Z. Anorg. Allg. Chem.* **2006**, *632*, 2164; c) B. Speiser, *Anal. Bioanal. Chem.* **2002**, *372*, 29–30.
[42] C. Daguenet, P. J. Dyson, I. Krossing, A. Oleinikova, J. Slattery, C. Wakai, H. Weingärtner, *J. Phys. Chem. B* **2006**, *110*, 12682–12688.
[43] H. K. Roobottom, H. D. B. Jenkins, J. Passmore, L. Glasser, *J. Chem. Ed.* **1999**, *76*, 1570–1573.
[44] H. D. B. Jenkins, H. K. Roobottom, J. Passmore, L. Glasser, *Inorg. Chem.* **1999**, *38*, 3609–3620.
[45] I. Krossing, L. Van Wüllen, *Chem. Eur. J.* **2002**, *8*, 700–711.
[46] A. Reisinger, W. Scherer, I. Krossing, unpublished results.
[47] T. E. Mallouk, G. L. Rosenthal, G. Müller, R. Brusasco, N. Bartlett, *Inorg. Chem.* **1984**, *23*, 3167–3173.
[48] L. Glasser, H. D. B. Jenkins, *Chem. Soc. Rev.* **2005**, *34*, 866–874.
[49] I. Krossing, J. M. Slattery, C. Daguenet, P. J. Dyson, A. Oleinikova, H. Weingärtner, *J. Am. Chem. Soc.* **2006**, *128*, 13427–13434.
[50] A. Carpy, M. Goursolle, J. M. Leger, E. Nivaud, *C. R. Acad. Sci. Ser. IIc* **1977**, *285*, 311.
[51] T. M. Miller, B. Berderson, *Adv. At. Mol. Phys* **1997**, 13.
[52] A. Bihlmeier, M. Gonsior, I. Raabe, N. Trapp, I. Krossing, *Chem. Eur. J.* **2004**, *10*, 5041–5051.
[53] R. Ahlrichs, M. Bär, M. Häser, H. Horn, C. Kölmel, *Chem. Phys. Lett.* **1989**, *162*, 165–169.
[54] A. D. Becke, *Phys. Rev. A* **1988**, *38*, 3098–3100.
[55] J. P. Perdew, K. Burke, Y. Wang, *Phys. Rev. B* **1996**, *54*, 16533–16539.
[56] P. Deglmann, F. Furche, R. Ahlrichs, *Chem. Phys. Lett.* **2002**, *362*, 511–518.

Received: March 7, 2008
Revised: November 26, 2008
Published online: January 8, 2009

